Analysis of Brush DC Equivalent Controlled Multiphase Cage Rotor Induction Machines

Nkosinathi Gule, MIEEE and Maarten J. Kamper, SMIEEE
E-mail: nathie@sun.ac.za, kamper@sun.ac.za

Abstract— **In a brush dc equivalent (BDCE) controlled machine, quasi-square like constant air gap flux density and rotor induced voltage waveforms are utilized. Analytical expressions for calculating the developed power, flux density, stator and rotor copper losses for the BDCE controlled cage rotor multiphase induction machine are developed in this paper. From analysing these expressions, it is found that, for a BDCE controlled machine with a certain torque and a certain flux density, there is a best (optimal) combination ratio of field to torque phases. Also, in this paper, measurement results in a prototype cage rotor multiphase induction machine drive are presented.**

I. INTRODUCTION

Multiphase induction machine drives possess several advantages over conventional three phase induction machine drives in high-power applications [1-10]. Besides better fault tolerance and higher reliability, the advantages of multi-phase induction machines include: (i) reduction in the: amplitude of torque pulsation, rotor harmonic currents, current per phase without increasing the phase voltage and dc link current harmonics, (ii) the increase in: machine power and torque per rms current for the same volume machine, and torque pulsation frequency. Depending on the stator winding, other advantages are: independent control of multimotor multiphase drive systems with a single power electronic converter supply and torque enhancement through stator current harmonic injection. Also, a higher phase number leads to the improvement of the quality of the air-gap flux density waveform regardless of the current waveform or winding design, because with a higher phase number there is less interaction between space and time harmonics.

Similarly to three phase induction machine drives, scalar control, vector control and direct torque control (DTC) have been used in the control of multiphase induction machine drives. Currently, more interest has moved towards vector and direct torque control (DTC) due to the higher cost of multiphase power electronics when compared to the cost of implementing control algorithms [4]. However, the vector and DTC control techniques are quite complex as coordinate transformations and model representation of the multiphase induction machine become more demanding with increase in the number of phases [1],[4].

A simple control method that does not require any coordinate transformation for multiphase induction machine drives was proposed and evaluated in [11-13]. This control method is in effect a direct implementation of the operation of a brush DC machine with compensating windings, i.e. the stator phase windings act alternately as flux or torque producing phase windings. For simplicity, this new method is called the brush dc equivalent (BDCE) control method. Similarly to other multiphase induction machine drives, the application of this drive utilising BDCE control is suitable for very-high-power variable speed drive applications, e.g. in the 50 MW power level, whereby the inverter current rating can be greatly reduced by using higher number of phases. The advantage possessed by BDCE control over vector control and DTC is its simplicity even for high number of phases, e.g. 15 phases.

In [11], the total number of phases are equally divided between torque and field phases, but, the question is: is this ratio necessarily the best, in terms of losses and inverter rating for a BDCE controlled machine with a certain torque and a certain flux density? In [12], a simple method of evaluating the optimal ratio of field to torque phases that answers this question is given. However, the reasons and benefits of why this ratio is necessary are not clearly stated or proved. Also, the results given are not evaluated practically through measurements.

In this paper, simple expressions for calculating the developed power, torque, stator and rotor copper losses of a BDCE controlled multiphase induction machine are developed. These expressions are investigated and used to prove that there is a need to fine the best combination of the field and torque phases in a BDCE controlled machine.

Furthermore, the BDCE control method utilising the optimally evaluated ratio of field to torque phases from [12] is evaluated on a 11 kW, nine-phase, cage rotor induction machine drive. Also, the effect on the ratio of the number of field (flux) to torque phases is investigated and confirmed through measurements.

II. BRUSH DC EQUIVALENT (BDCE) CONTROL METHOD

The principle of operation of the BDCE multiphase induction machine drive is best explained graphically. The configuration of the stator phase current waveforms shown in Fig. 1 allows separate rotating flux or field MMF with an amplitude, F_f, and a torque MMF with an amplitude, F_t, in a two pole six-phase induction machine. Thus, the stator phase current consists of trapezoidal-shaped field and torque current components, with flat-topped amplitudes of I_f and I_t respectively. That is, a stator phase acts alternately in time as either a flux or a torque producing phase. Furthermore, it can be seen from Fig. 1 and Fig. 2 that at any instant there are always three neighbouring stator phase windings that act as field windings to generate the flux in the machine whilst the other three neighbouring stator phase windings always act as torque wind-

978-1-4673-6392-1/13/$31.00 ©2013 IEEE

ings to generate the torque of the machine. The generated flux in the machine will lead to induced rotor phase voltages and currents at slip speed. The rotor currents produce the rotor MMF, F_r. The torque current flowing in the torque producing stator phases, however, produces a counter MMF that balances the rotor MMF during operation of the BDCE controlled multiphase induction machine.

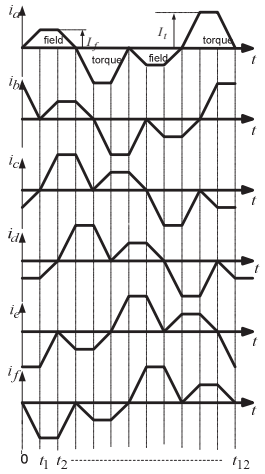

Fig. 1. Trapezoidal six-phase current waveforms [11].

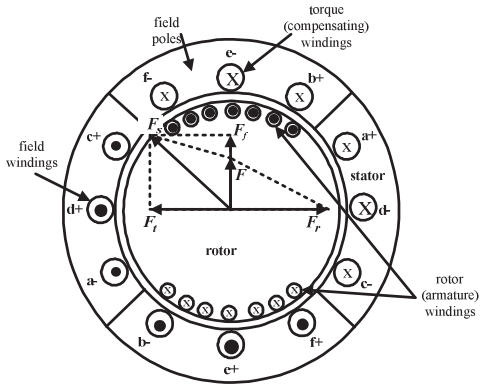

Fig. 2. Current distribution and MMF space phasors at time $t = t_1/2$ of the waveforms of Fig. 1.

Thus as shown in Fig. 2, with $F_t = F_r$ the balanced MMF condition (flux decoupling condition) is achieved. There is, thus, an important relationship between the torque current, I_t, and the angular slip frequency, ω_{sl}, for balanced MMF control (or decouple control), that is

$$k = \frac{\omega_{sl}}{I_t}. \tag{1}$$

The relationship given by (1) is used in the control system, where k is used as a control gain. The control gain, k, also depends on the physical dimensions of the machine, the total number of phases, the rotor phase resistance and the air-gap flux density as is given in the next section.

Fig. 3 shows a block diagram of an N_p-phase induction machine drive with its control system. Similarly to [14] and to phase redundant multiphase systems [2], a full bridge inverter is used for each stator phase winding, which results in $2N_p$ phase legs for a N_p-phase drive. The rotor speed together with the phase currents of the drive are measured and fed back to a digital signal processor (DSP) controller. The field current is kept constant under base speed. The speed controller controls the torque-command current I_t^* from which the slip angular frequency ω_{sl} is determined using the control gain, k, of (1). From this and from the known field-command current I_f^*, the N_p reference phase currents of the drive are generated. In this case, a digitally implemented hysteresis current regulator, using a field programmable gate array (FPGA), is used for the current control. The switching signals are sent to the inverter via fibre optic cables. The advantage of this control method is that it does not require any transformations and model representations such as in vector control and DTC.

III. Theoretical Analysis

A. Developed power and torque

Similarly to the induced rotor phase voltage, the stator phase voltage is square-like. The flat-topped induced voltage value per stator phase is given by,

$$\begin{aligned} E_s &= 2N_s l r_g B \omega_r \\ &= K_1 B \omega_r, \end{aligned} \tag{2}$$

where, ω_r is the rated speed of the machine and K_1 is a constant. Since ω_r is at rated speed for rated power, that is, E_s is constant, then from (2), B is also a constant. B is given by,

$$\begin{aligned} B &= \frac{\mu_0 F_f}{g k_c k_s} = \frac{\mu_0 N_s \left(m_f - 1\right) I_f}{2 p g k_c k_s} \\ &= K_2 \frac{\left(m_f - 1\right) I_f}{k_s}, \end{aligned} \tag{3}$$

where, g is the air-gap length, K_2 is a machine constant, k_s is the saturation factor and k_c is the Carter factor. Rearranging (3) leads to

$$I_f (m_f - 1) = \frac{k_s}{K_2} B, \tag{4}$$

or,

$$I_f (m - m_t - 1) = \frac{k_s}{K_2} B. \tag{5}$$

It can be seen from (4) and (5) that, increasing m_t leads to a decrease in m_f and an increase in I_f. In the machine, if m_f is reduced, the flux per pole increases (as B is constant whilst the pole area increases) and saturation increases in the stator and rotor yokes, thus, k_s in (5) increases, which leads to I_f increasing even more (due to saturation) to maintain the balance of (5). Thus, care must be taken in selecting m_t for a particular machine.

The developed power, P_n, of a BDCE controlled multiphase induction machine is,

$$P_n = \left(m_t - 1\right) E_s I_t, \tag{6}$$

Rearranging (6) leads to

$$\left(m_t - 1\right) I_t = \frac{P_n}{E_s}. \tag{7}$$

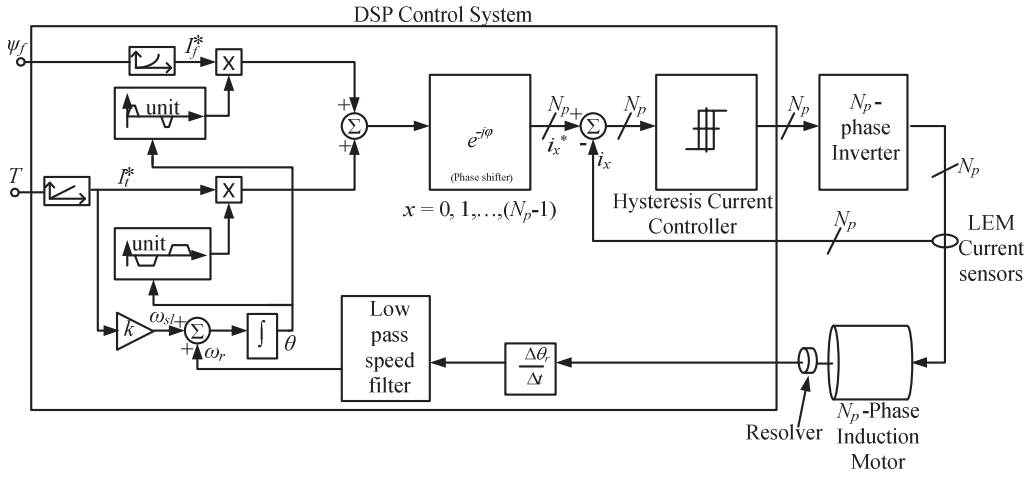

Fig. 3. BDCE control system of a N_p-phase induction motor.

The right hand side of (7) is a constant since P_n is equal to the rated power of the machine and E_s is equal to the rated voltage of the machine and thus, a decrease in I_t leads to a proportional increase in (m_t - 1) or vice versa. Also from (6), it is seen that, the more the m_t, the lower is I_t and the lower the power rating per phase. Thus, it can be seen at this stage that theoretically m_t should be as large as possible, that is, $m_t = m$ - 3.

From (6) and (2), the rated torque of the machine, T, is given by,

$$T = \frac{P_n}{\omega_r} = K_1 (m_t - 1) B I_t . \tag{8}$$

Substituting for B from (3) in (8) gives,

$$T = \frac{K_2 K_1}{k_s} (m_t - 1)(m_f - 1) I_f I_t . \tag{9}$$

In (9), with the relations between I_f and (m_f -1), and between I_t and (m_t - 1) as described above, T is constant.

B. *Inverter currents and stator slot current density*

The rated values of the field and torque current amplitudes determine the current rating of the IGBT switches to be used in the inverter. In some cases, the difference between I_f and I_t may be large and the IGBT may then be under-utilised during some time instances and over-utilised during others. For the same rating machine and with the total number of stator phases kept constant, the possible stator current waveform shapes are shown in Fig. 4 *a)*, *b)* and *c)*. In Fig. 4 *a)*, the number of field and torque phases are equal whilst $I_t > I_f$. Here, only half of the time the inverter switches are operating at full (rated) current potential. For some cases, $I_t = I_f$ (Fig. 4 *b)*) or $I_t < I_f$ (Fig. 4 *c)*). From Fig. 4, it is clear that in the case of current waveforms *a)* and *c)*, the peak stator slot current density varies during a cycle (period), whilst in the case of *b)*, it stays constant. This has a bearing on the cooling of the machine. Thus, it is clear that, I_t must be as close as possible to I_f in order to allow for efficient inverter rating selection, inverter usage and the cooling of the machine.

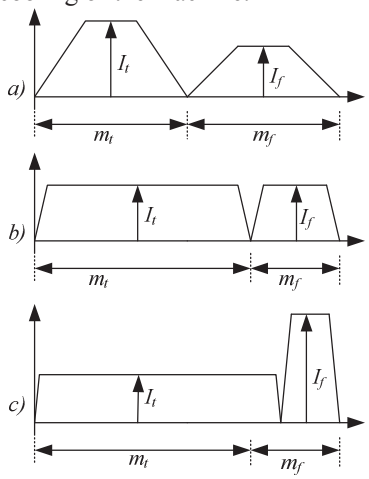

Fig. 4. Possible stator current waveform shapes for a BDCE-controlled multi-phase induction machine (only half a period of the waveform is shown). *a)* $m_t = m_f$ and $I_t > I_f$, *b)* $m_t > m_f$ and $I_t = I_f$, *c)* $m_t > m_f$ and $I_t < I_f$.

C. *Stator copper losses*

In Fig. 5, only the torque component of a stator phase current is shown. During drive operation, at any time instance, there are (m_t - 2) torque phases carrying the rated current I_t, whilst two torque phases are in a transition stage (one with increasing and the other with decreasing I_t versus time). The instant positions of the two phases in a transition stage are labelled as u and (1 – u) in Fig. 5, where u varies between 0 and 1.

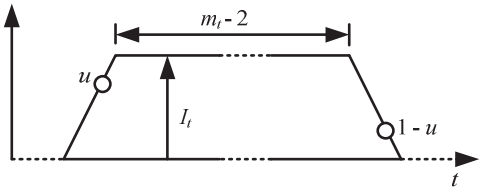

Fig. 5. Single stator phase current waveform torque component

For ease of calculation, the stator copper loss of the torque phases at each time instance are separately calculated for the (m_t - 2) torque phases and for the two phases in a transition phase. The copper loss of the (m_t - 2) torque phases is

$$P_{tcu1} = (m_t - 2) I_t^2 R_s , \tag{10}$$

while the copper loss for the two phases in a transition stage is

$$\begin{aligned} P_{tcu2} &= u I_t^2 R_s + \left[(1-u) I_t\right]^2 R_s \\ &= I_t^2 R_s \left(2u^2 - 2u + 1\right), \end{aligned} \tag{11}$$

where R_s is the stator phase resistance and u is the position on the slope of the waveform varying between 0 and 1 as shown in Fig. 5. In Fig. 6, the plot of the function $2u^2 - 2u + 1$ is shown. It can be seen in the figure that the minimum of the function is when the currents flowing in the two torque phases in the transition stage are equal at $u = 0.5$.

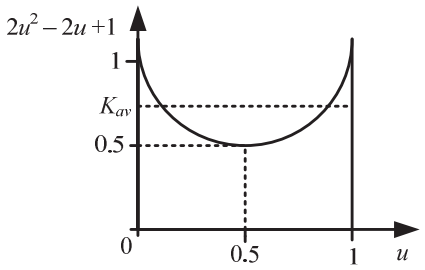

Fig. 6. $2u^2 - 2u + 1$ function plot.

From (10) and (11), the total instantaneous copper loss of the torque phases is calculated as

$$\begin{aligned} P_{tcu} &= P_{tcu1} + P_{tcu2} \\ &= (m_t - 2) I_t^2 R_s + I_t^2 R_s \left(2u^2 - 2u + 1\right). \end{aligned} \tag{12}$$

From (12), the average copper loss of the torque phases is

$$P_{tcu} = \left[(m_t - 2) + K_{av}\right] I_t^2 R_s , \tag{13}$$

where K_{av} is the average of the function ($2u^2$ - $2u$ + 1), as shown in Fig. 6 and is determined as,

$$\begin{aligned} K_{av} &= \int_0^1 (2u^2 - 2u + 1) du \\ &= \frac{2}{3}. \end{aligned} \tag{14}$$

It must be noted that the value of K_{av} is the same irregardless of the number of torque phases. Similarly, the average copper loss of the field phases can be shown to be

$$P_{fcu} = \left[(m_f - 2) + K_{av}\right] I_f^2 R_s . \tag{15}$$

Thus the total stator copper loss, P_{scu}, is

$$\begin{aligned} P_{scu} &= P_{tcu} + P_{fcu} \\ &= \left[(m_t - 2) + K_{av}\right] I_t^2 R_s + \left[(m_f - 2) + K_{av}\right] I_f^2 R_s , \end{aligned} \tag{16}$$

or,

$$P_{scu} = \left[m_t - 2 + K_{av}\right] I_t^2 R_s + \left[m - m_t - 2 + K_{av}\right] I_f^2 R_s . \tag{17}$$

Hence, the minimum value of the stator copper losses can be found by differentiating (17) with respect to m_t, that is,

$$\frac{dP_{scu}}{dm_t} = I_t^2 R_s - I_f^2 R_s = 0 . \tag{18}$$

This implies that the minimum value of the stator copper loss is found when

$$I_f = I_t . \tag{19}$$

It is significant that this result is in agreement with the requirement for the inverter currents as previously stated in section *B*. Alternatively, the total stator copper losses can be calculated as

$$P_{scu} = I_{srms}^2 R_s m , \tag{20}$$

where, I_{srms} is defined as the rms value of the stator current waveform.

The equivalence of the total stator copper loss expressions given by (17) and (20) can be verified by means of an example. Consider a BDCE controlled induction machine with parameters as given in Table 1. For each combination of m_f and m_t, the corresponding value of I_f and I_t is calculated from (5) and (8) respectively as given in Table 2. Saturation is assumed constant in the calculation of I_f, and the saturation factor is taken as, k_s = 1.0. Also, the ratios, P_{scu}/R_s, calculated from (17) and (20) are given and compared in the table. It can be seen from Table 2 that the minimum value of P_{scu}/R_s is obtained when $I_f \approx I_t$, as also found in (19). The results show that (17) can be used to calculate the stator copper losses in a simple and fast way.

TABLE 1. 12 PHASE, 31.4 KW MACHINE PARAMETERS

T	200 Nm
N_s	85 turns
l	0.13 m
r_g	0.35 m
B	0.7 T
p	2
g	0.0005 m
k_c	1.2
m	12

TABLE 2. CALCULATED VALUES OF I_T, I_F AND P_{SCU}/R_S FOR A 12-PHASE MACHINE

m_f	6	5	4	3
m_t	6	7	8	9
I_t (A)	7.39	6.16	5.28	4.62
I_f (A)	3.15	3.93	5.24	7.86
P_{scu}/R_s (17) (W/Ω)	300.89	271.48	258.95	266.55
P_{scu}/R_s (20) (W/Ω)	300.89	271.48	258.95	266.55

D. Rotor copper losses

The induced rotor phase or bar current is directly proportional to the slip speed, ω_{sl}, and according to (1), ω_{sl} is directly proportional to I_t since the control gain, k, is constant irregardless of the number of torque phases. Thus, decreasing I_t (that is, increasing m_t) results in a decrease in the peak bar current density and a decrease in the copper losses per bar. Thus, better machine cooling is obtained as lower peak currents flows in the rotor bar. Under balanced MMF conditions (proper BDCE control), $F_t = F_r$. With

$$F_t = \frac{1}{2}(m_t - 1)\left(N_s / p\right) I_t \tag{21}$$

and

$$F_r = m_{ra} N_r I_r , \tag{22}$$

the rotor bar current is given by

$$I_r = \frac{(m_t - 1) N_s I_t}{2 p m_{ra} N_r}, \tag{23}$$

The total rotor bar copper losses (for the active bars) can be calculated as

$$\begin{aligned} P_{rcu} &= 2 p m_{ra} I_r^{\,2} R_b \\ &= \frac{(m_t - 1)^2 N_s^{\,2} I_t^{\,2}}{2 p m_{ra} N_r^{\,2}} R_b , \end{aligned} \tag{24}$$

where R_b is the bar resistance. Using (8) it can be shown that (24) becomes

$$P_{rcu} = \frac{R_b N_s^{\,2} T^2}{2 p m_{ra} N_r^{\,2} K_1^{\,2} B^2}, \tag{25}$$

where T, R_b and B are constants. Since

$$m_{ra} = \frac{M_r (m_t - 1)}{2mp}, \tag{26}$$

it can be seen, from (25), that the total rotor copper losses for a specified rated machine, under BDCE control, depends on the number of active rotor bars, m_{ra}, which, in turn depends on m_t from (26). Thus, an increase in m_t will lead to a decrease in P_{rcu}.

Thus, from this section, it is noted that in any machine under BDCE control, care needs to be taken in selecting the m_t and m_f combination, as this directly affects the inverter rating, stator and rotor copper losses and saturation in the machine. The best combination ratio m_f/m_t is defined as the ratio that provides $I_f \approx I_t$, and limits saturation in the stator and rotor yokes. Note that this ratio is evaluated with P_n, T, B, m and p kept constant. A method of calculating the best ratio is given in [12].

IV. Nine-phase Cage-Rotor Induction Machine Drive Evaluation

A nine-phase cage rotor induction machine drive is developed using the proposed control method of Section II. A cage rotor is specifically selected in this case.

A standard 11 kW, four-pole, 36-slot, three-phase induction machine stator is rewinded to a nine-phase stator with full-pitch (concentrated) coils. The original 28-slot cast aluminium cage rotor of the three-phase induction machine is used for the rotor of the nine- phase induction machine. Additional parameters of the nine-phase machine are given in Table 3.

The nine-phase inverter comprises of Intelligent Power Modules (IPMs), the control and isolated power circuits, the dc bus bar and per phase current sensors. Modular design is utilised in the design of the inverter since it allows for independent testing and simple replacement of faulty boards. An H-bridge is required for each phase of the nine-phase machine, thus, the inverter consists of six 6MBP25RA120 three-phase intelligent power modules (IPMs). Each control board is shared by two IPMs. The hardware and software of the DSP system of Fig. 3 is expanded to become a nine-phase control system. The nine-phase trapezoidal stator current waveforms are generated similarly to the six-phase waveforms described in section II. The optimal (best) ratio of the number of field phases to torque phases,

$$m = \frac{m_f}{m_t}, \tag{27}$$

is calculated for the 9-phase machine as $m = 0.5$ (that is, $m_f = 3$ and $m_t = 6$), which is in contrast with $m = 1$ ($m_f = 3$ and $m_t = 3$) that is used in [11].

V. Results

The percentage efficiency of the drive system (converter and induction motor) is calculated as the percentage ratio of the output (shaft) power to the input (ac) power. The input power is measured with a power analyser at the ac supply of the converter. Fig. 7 shows the measured percentage efficiency versus percentage load. The percentage load is calculated as the percentage ratio of the measured torque to the rated torque. The figure shows that there is a slight gain in efficiency when less field phases are used similar to what was observed in section III. Furthermore, the nine-phase induction machine drive system compares well, in terms of efficiency, to the standard three-phase drive system under constant volt per hertz operation as shown in the figure; a Danfoss drive is used in this case to supply the three-phase induction machine. The per phase stator current waveforms for different number of field and torque phase combinations are shown in Fig. 8, at rated flux and load. Here, the negative (un-equal) effect of the (m_f,m_t) = (4,5) winding option on the torque and field converter currents compared to the (m_f,m_t) = (3,6) winding option, can be clearly seen.

TABLE 3. MACHINE PARAMETERS OF A 4-POLE 9-PHASE INDUCTION MACHINE.

Rated Power, P_n	11kW
Air-gap length, g	0.5 mm
Stack length, l	127 mm (copper bars)
Stator radius	130 mm
Rotor radius, r_g	84.5 mm
End ring segment resistance, R_e	1.28e-6 Ω (75°C)
End ring segment inductance, L_{er}	29.2 nH
Number of field phases, m_f	3
Number of torque phases, m_t	6
Number of rotor bars, M_r	28
Number of stator slots, M_s	36
Number of series turns per stator	170
Air-gap flux density, B	0.7 T
Rated I_f	5.83 A
Rated I_t	5.5 A
Rated k	0.638 rad/As
Rated speed	1466 r/min

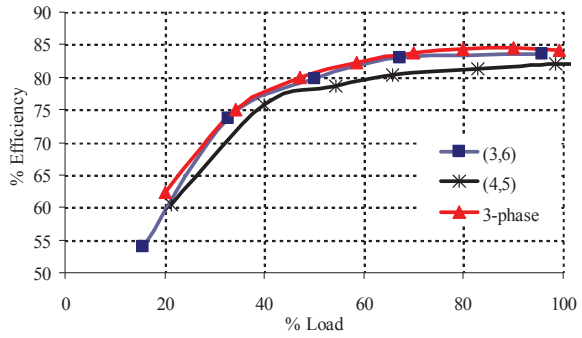

Fig. 7. Measured system (converter and motor) efficiency versus percentage load of the nine-phase induction machine drive compared to a conventional three-phase induction machine drive, with (m_f,m_t) a parameter. (Rotor speed = 1500 r/min and at rated dc bus voltage of V_{dc} = 400 V)

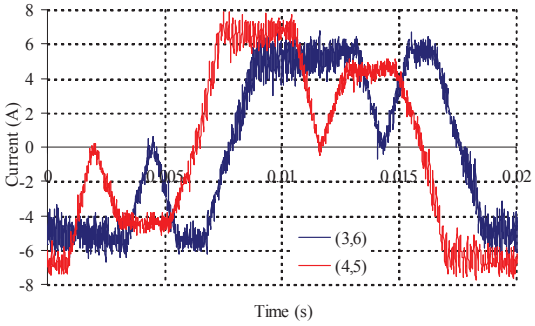

Fig. 8. Measured stator current waveforms at rated flux and rated torque, with (m_f,m_t) a parameter and k = 0.638. For (3,6), I_f = 5.83 A and I_t = 5.5 A, whilst, for (4,5), I_f = 4.68 A and I_t = 6.83 A. The dc bus voltage for this measurement is, V_{dc} = 400 V and the rotor speed is 1500 r/min.

VI. CONCLUSION

In this paper, analytical expressions of calculating the developed power, torque, stator and rotor copper losses of the BDCE controlled machine are presented. Based on analysing these expressions, it is found that there is a best/optimal ratio of field to torque phases of multiphase induction machines under BDCE control. With fewer field phases, there is increased rotor winding utilization and more torque phases can be used. The measured value of the percentage efficiency of the BDCE controlled nine-phase induction machine drive compares well with the three-phase volt/hertz controlled off-the-shelf drive. Also, better inverter current rating, in terms of the amplitudes of the field and torque currents, is achieved when fewer field phases are used. Thus the developed expressions and the developed criterion of calculating the optimal ratio of field to torque phases can be used in the design of BDCE controlled multiphase induction machines.

REFERENCES

[1] E. Levi, "Recent Developments in High Performance Speed Multiphase Induction Motor Drives," in Sixth International Symposium Nikola Tesla, 2006.

[2] G. K. Singh, "Multi-Phase Induction Machine Drive Research - A survey," Elsevier Electric Power Systems Research, pp. 139-147, 2002.

[3] H. A. Toliyat and T. A. Lipo, "Analysis of Concentrated Winding Induction Machines for Adjustable Speed Drive Applications-Experimental Results," IEEE Transactions on Energy Conversion, vol. 9, pp. 695-700, December 1994.

[4] E. Levi, R. Bojoi, F. Profumo, H. A. Toliyat, and S. Williamson, "Multiphase Induction Motor Drives - A Technology Status Review," IEE Proceedings - Electric Power Applications, vol. 1, pp. 489-516, July 2007.

[5] A. C. Smith, S. Williamson, and C. G. Hodge, "High torque dense naval propulsion motors," in Proc. IEEE International Electric Machines and Drives Conference IEMDC, 2003, pp. 1421–1427.

[6] M. Jones, S. N. Vukosavic, and E. Levi, "Parallel-Connected Multiphase Multidrive Systems With Single Inverter Supply," IEEE Transactions on Industrial Electronics, vol. 56, pp. 2047 - 2057, 2009.

[7] H. Xu, H. A. Toliyat, and L. J. Petersen, "Rotor field oriented control of five-phase induction motor with the combined fundamental and third harmonic currents," in 16th Annual IEEE Applied Power Electronics Conference and Exposition, APEC 2001, 2001.

[8] R. O. C. Lyra and T. A. Lipo, "Torque Density Improvement in a Six-Phase Induction Motor With third Harmonic Current Injection," IEEE Transactions on Industry Applications, vol. 38, pp. 1351-1360, 2002.

[9] G. W. McLean, G. F. Nix, and S. R. Alwash, "Performance and design of induction motors with square-wave excitation," IEE Proceedings, vol. 116, pp. 1405 - 1411, 1969.

[10] H. A. Toliyat, T. A. Lipo, and J. C. White, "Analysis of a Concentrated Winding Induction Machine for Adjustable Speed Drive Applications: Part 1 (Motor Analysis)," IEEE Transactions on Energy Conversion, vol. 6, pp. 679-683, 1991.

[11] Y. Ai, M. J. Kamper, and A. D. L. Roux, "Novel Direct Flux and Direct Torque Control of Six-Phase Induction Machine with Nearly Square Air Gap Flux Density," IEEE Transactions on Industry Applications, vol. 43, pp. 1534-1543, December 2007.

[12] N. Gule and M. J. Kamper, "Optimal Ratio of Field to Torque Phases in Multi-Phase Induction Machines Using Special Phase Current Waveforms," in Proceedings of International Conference on Electrical Machines (ICEM2008), 2008.

[13] N. Gule and M. J. Kamper, "Multi-phase Cage Rotor Induction Machine with Direct Implementation of Brush DC Operation," in International Electric Machines and Drives Conference (IEMDC2011) Niagara Falls, Canada, 2011.

[14] L. Weichao, H. An, G. Shiguang, and S. Chi, "Rapid Control Prototyping of Fifteen-Phase Induction Motor Drives Based on dSPACE," in International Conference on Electrical Machines and Systems, ICEMS 2008, 2008.